ICMIEE22-042

Effect of Blockage Area Variation on the Hemodynamic Characteristics in Stenosed Artery using Numerical Techniques

B. M. Arafat Rahman[1,*], Ahmed Abrar Shayor[2], Abdullah Al-Faruk [3]
[1] Department of Mechanical Engineering, Khulna University of Engineering & Technology, Khulna-9203, BANGLADESH
[2] Department of Mechanical Engineering, Khulna University of Engineering & Technology, Khulna-9203, BANGLADESH
[3] Department of Mechanical Engineering, Khulna University of Engineering & Technology, Khulna-9203, BANGLADESH

ABSTRACT

The investigation and in-depth study of vascular fluid dynamics play a critical role in the inquiry of how the progression of atherosclerosis occurs, a large prominent disease in humans. Recent evolution in computational fluid dynamics (CFD) is allowing contribution to monitoring flow in presence of stenosis without in-vivo techniques with sufficient accuracy and less cost. Computer-based medical imaging techniques and mainly simulating complex flows would also help in developing therapeutics and devices to detect the stenosis severity in advance using values of velocity, pressure, and other hemodynamics parameters. In the present work two-dimensional artery models with single stenosis but with blockage percentages of 35%, 50%, 75%, 80%, 86%, and 95% respectively were taken for carrying out the analysis, a numerical simulation was hence performed to assess the effect on physiological flows. The blood is stipulated to be incompressible, homogenous, and non-Newtonian, while the artery is fixed and rigid. The continuity, momentum, and standard k-ω turbulence equations, as well as the non-Newtonian Carreau model, will be used to describe the flow field in the mathematical model. Steady-state analysis was carried out for the case since simple instantaneous analysis does not warrant a complex transient flow study. The velocity profile, wall static pressure, wall shear stress, and turbulence intensity were measured in pre-stenotic, throat, and post-stenotic regions. At the throat, the flow changes rapidly, causing an escalation in velocity and wall shear stress (WSS) deviating from flow in the normal artery. In the post-stenotic region, the flow is quite turbulent, resulting in the creation of vortices. The results indicated that the blockage caused the development of high velocity and along with the viscosity change causes high WSS to develop on the wall. Because of the stenosis, the throat section has a significant pressure variation and flow becomes turbulent due to crossing the critical Reynolds number. Also, it was found from the investigation that a 75 % blockage is dangerous enough and 80% stenosis can be considered critical. This characterization of criticality was performed by studying the turbulence intensity variable of the flowing biofluid (blood).

Keywords: CFD, Blood Flow, Stenosis, Blockage Area, Turbulence Intensity

1. Introduction

The inflammatory fibroproliferative response to numerous morphs of endothelial injury is classified as atherosclerosis, an arterial disease [1]. A fractional decrease in the artery cross-sectional area, known as stenosis, in atherosclerosis [2]. Atherosclerosis damages arteries throughout the body. Atherosclerotic lesions are most found in arterial sections with steep curvature or at bifurcations and junctions, where they cause significant changes in flow structure [3]. Although the exact causes of this anomaly are still unknown, it has been established that once modest stenosis develops, the ensuing flow disruption plays a critical part in the disease's advancement [4].In addition to traditional medical methods for theorizing and assessing disease progression, computational fluid dynamics is being used to investigate the role of hemodynamics in the regionalization, growth, and advancement of atherosclerosis disease in the study of the reasons and amelioration of this disease. Some researchers have concentrated on modelling the arterial wall and examining the association between arterial wall stress and vascular wall disorders at the same time as hemodynamic investigations [5], [6].

Researchers have recently focused on biological systems incorporating fluid-solid interactions in them, particularly cardiovascular systems. They anticipate that combining fluid and solid solutions will aid in better grasping the trend of vascular disease [7]. Bathe et al. (1999), used ADINA Software was used to model pulsatile and laminar flow through a flexible artery with stenosis. They looked at stenoses with an area reduction of 51 and 96 per cent and compared pressure drop and circumferential stress across the artery at different instances. They also looked at how the Reynolds number (Re) affects pressure descent [8]. Tang et al. (1999), Using ADINA software, investigated flexible carotid arteries with laminar flow involving symmetric stenosis. Severe stenosis generates critical flow circumstances including negative pressure gradient and high and low shear stress, which can lead to artery compression, plaque rupture, platelet activation, and arterial thrombosis, according to their findings [9]. Many experiments have been conducted to examine a steady turbulent flow [10]–[11]. Deshpande et al. (1980), used a Laser Doppler Anemometer (LDA) to study chaotic(turbulent) flow through a stenosed tube with 75% reduction and Re ranging from 5000 to 15000 [12]. Ahmed et al. (1984), used the LDA to determine the simplified time-independent velocity field in the presence of symmetric stenosis having stiff walls. At upstream of the stenosis, Re ranged from 500 to 2000, and stenoses of 25, 50, and 75 per cent diameter decrease were investigated [11]. Few experimental investigations for unstable turbulent

* Corresponding author. Tel.: +88-01721961399
E-mail addresses: bmarafatrahman@gmail.com

flow due to the existence of stenosis exist due to the difficulty of conducting experiments.[12]

Ahmed et al. (1984), measured the pulsating flow field hypothesizing, and implementing symmetric stenosis by LDA. For testing, they used a sinusoidal inlet velocity profile, 7.5 Womersley number, stenoses of 25, 50, and 75% blockage, and a mean Reynolds number of 600 [13]. Transient or turbulent flow can occur even with a minor percentage of stenosis, according to these experiments. Results of the preceding experiments were employed to check numerical approaches for simulating turbulent flow in interior flows using the finite element program FIDAP for example. Ghalichi et al. (1998), evaluated time dependent and turbulent flow. Their findings revealed that when the flow becomes transitional or turbulent, the laminar flow model overstates the vortex length [14]. Kader and Shenory et al. (2011), numerical simulation findings demonstrate that increasing the degree of stenosis enhances the velocity and stenotic jet length. Their findings also show that the 3D stenotic CFD model competently forecasts shifts in flow behavior with increasing degree of the stenosis [15].

Tu et al. (1996), performed a finite element numerical analysis in an artery with a rigid wall, evaluating steady and unsteady blood flow through 25, 50, and 75% stenosis [16]. Tu et al. (1996), used the Herschel–Bulkley model and evaluated the non-Newtonian (varying viscosity, physiological pulsatile blood flow through heavy stenosis. [16]. Razavi et al. (2011), conducted a comparison of other viscosity models as well as the Newtonian model. They concluded that as the percentage of stenosis grows, the flow downstream of stenosis gets more disrupted, and WSS formation at the throat region becomes more noticeable [17]. Ellahi et al. (201An analytical investigation of a incompressible, pulsatile flow of micropolar non-Newtonian fluid was done in a stenosed artery. They discovered that when the stenosis height grows, so does the flow impedance [18]. Karimi et al. (2013), used a 3D model adopting axisymmetric stenosis conditions in common carotid artery to visualize the hemodynamical differences between 2D axisymmetric and 3D models in pulsatile blood flow, employing Carreau with Modified Power-law models, later Newtonian model as well. Discovery of asymmetric flow in the post stenosis zone, which can only be seen through 3D modelling was found [19]. Harloff et al. (2013), used imaging in the 4D technique to study flow velocity within a stenosed artery [20]. Additionally, in recent years, certain researchers, such as Saleem et al. (2014), have made significant contributions to the blood flow modeling field in stenosed arteries [21].Tian et al. (2013) computationally simulated non-Newtonian models with pulsatile velocity across a stenosed artery including varying degrees of severity and impact on the WSS magnitudes, wall shear stress gradient (WSSG), and other parameters on both walls, however the lower wall had a much higher WSSG [22].Shupti et al. (2017) worked with non-Newtonian fluid flow and moving wall, researched into the relationship between stenosis and aneurysm [23].Lorenzini et al. (2008), examined stenoses with various geometric profiles such as trapezium, semi-ellipse, and triangle in terms of non-Newtonian behavior. [24]. Flow features in the proximal and distal end of stenosis have been studied in some of the prior experimental and computational research studies, including a full investigation of the rupture potential of plaque. Aside from that, the flow patterns with increasing severity have been widely researched for various geometry along with different kinds of physiological models. In the current study, an attempt was carried out to demonstrate the substantial changes for several severities considering blood is homogeneous, incompressible, and non-Newtonian. During a cardiac cycle, the shear rate in human arteries fluctuates from 1–1200 s^{-1} [25]. As a result, blood behaves like non-Newtonian fluid at times during the cardiac cycle. To completely comprehend hemodynamics, necessary investigate into the non-Newtonian behavior of blood is required.

The flow is considered steady. For large arteries, the steady flow assumption is reasonable since diastole, which lasts about two-thirds of the cardiac cycle, has a reasonably constant forward flow [26].

2. Model Description

The model description including the geometry, mesh, numerical studies are explained in detail as follows. It is to be mentioned that the modelling is being done for systematic circulation of blood flow.

2.1. Geometry

The form of the stenoses chosen for this study is

$$\frac{r(x)}{D} = 0.5 - A[1 + \cos\ \pi x/D], -D \leqslant x \leqslant D$$

with $x = 0$ exactly at the middle of throat of stenosis and D is artery diameter. By considering D as reference length while making it dimensionless we get 1 non-dimensional form. Usually, the artery size is about 4 mm [27]. The stenosed percentage is found from $[1 - (r/R)^2]$, The throat and upstream arterial radius, are represented by r and R respectively. To guarantee fully developed upstream flow, a velocity profile was imposed 8 diameters (D) before $x = 0$ position. To allow for the reconstruction of flow, the outlet boundary condition was placed 20 diameters (D) downstream of the stenosis throat. **Fig.1** shows the geometry for 75% stenosis. And Error! Reference source not found. shows the value of r a nd A for various percentages of stenosis.

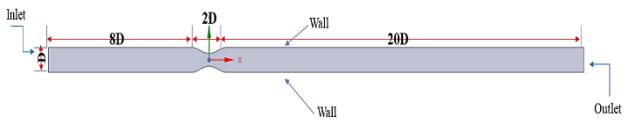

Fig.1 Geometry Description

Table 1 r and A for various percentages of stenosis

Stenosed Percentage	r	A
35%	0.4031	0.0485
50%	0.354	0.073
75%	0.25	0.125
86%	0.187	0.1565
95%	0.1118	0.19425

2.1 Mesh Generation

In this step, the geometrical model is discretized into various infinitesimally small volumes. Number of elements and nodes created for each geometry are shown in **Table 2**.

Table 2 The number of nodes and elements generated in each geometry

Model Name	Nodes	Elements
2D Stenosed Artery	122206	120700

Edge sizing and Face meshing has been done for this geometry. For edge sizing geometry has been divided into 3 sections with the longest section being pre-stenotic and shortest the stenotic region. In pre stenotic section the number of divisions has been taken 360. At the stenotic throat the number of divisions has been taken 160(finest to capture better flow physics as flow reach transitional stage). The post stenotic region the number of divisions has been taken 900(also finer to capture more flow physics as flow becomes turbulent. And at inlet and outlet the number of divisions has been taken 85 with a biasing factor 15 for reducing element size at near wall for better results. The mesh behavior has been taken as Hard. For Face Meshing elements type has been taken as quadrilaterals as can be perceived from **Fig.2**.

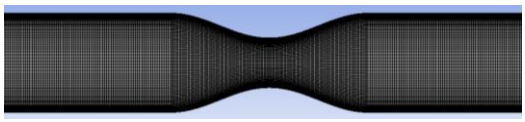

Fig.2 Meshing of the geometry

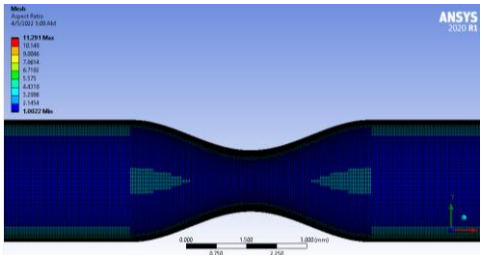

Fig.3 Aspect Ratio of the Mesh Elements

The Aspect Ratio, Skewness and Orthogonal Quality of mesh has been monitored closely for analyze the Mesh quality. As from **Fig.3** We can see that most of the areas the aspect ratio is equal to 1. In the boundary layer its value is higher than 1. But in boundary layer we need skewed layers of mesh as they are more stretched but with less height. The skewness for most of the elements close to 0 and (maximum 0.85). So, the Skewness property is very good along with the orthogonal qualities are also very satisfactory as most of the element has orthogonal quality value as 1.

2.2. Blood Properties

The fluid (blood) is considered homogeneous, incompressible, and non-Newtonian. The mass density of blood is considered as 1060 Kgm^{-3}. The flow is considered as steady. For Non-Newtonian fluid, according to Pierre Carreau's suggested Carreau model-

$$\mu = \mu_\infty + (\mu_0 - \mu_\infty)[1 + (\gamma_c \dot{\gamma})^2]^{n-1/2} \quad (1)$$

Where $\mu_\infty = 0.0035$ Pa a.s, $\mu_0 = 0.056$ Pa. $s, \gamma_c =$ 3.313 s, $\dot{\gamma}$ is the instantaneous shear rate, and n=0.356

2.3 Governing Equations

Continuity Equation:

$$\frac{\partial \rho}{\partial t} + \frac{1}{r}\frac{\partial (r\rho u_r)}{\partial r} + \frac{1}{r}\frac{\partial (\rho u_\theta)}{\partial \theta} + \frac{\partial (\rho u_z)}{\partial z} = 0 \quad (2)$$

Since the problem is assumed to be steady-state & incompressible, so time-dependent parameter ($\frac{\partial \rho}{\partial t}$) & ρ dropped from the equation & get,

$$\frac{1}{r}\frac{\partial (r u_r)}{\partial r} + \frac{1}{r}\frac{\partial (u_\theta)}{\partial \theta} + \frac{\partial (u_z)}{\partial z} = 0 \quad (3)$$

Navier's Stock equation. It mostly deals with fluid velocity and pressure parameters. We can calculate the flow characteristics by utilizing various boundary conditions. Incompressible and incompressible flows, both the momentum and Bernoulli's equations are applied. They are mostly intended for streamlined computations. The total of forces operating on a fluid body element to its accelerating rate of change of momentum is depicted by the momentum equation.

In cylindrical coordinates, (r, θ , z) the Navier-stokes incompressible fluid's equation of motion, with a constant dynamic viscosity μ and density ρ are:

$$\rho\left[\frac{Du_r}{Dt} - \frac{u_\theta^2}{r}\right] = -\frac{\partial p}{\partial r} + f_r + \mu\left[\nabla^2 u_r - \frac{u_r}{r^2} - \frac{2}{r^2}\frac{\partial u_\theta}{\partial \theta}\right] \quad (4)$$

$$\rho\left[\frac{Du_\theta}{Dt} + \frac{u_\theta u_r}{r}\right] = -\frac{1}{r}\frac{\partial p}{\partial \theta} + f_\theta + \mu\left[\nabla^2 u_\theta - \frac{u_\theta}{r^2} + \frac{2}{r^2}\frac{\partial u_r}{\partial \theta}\right] \quad (5)$$

$$\rho\frac{Du_z}{Dt} = -\frac{\partial p}{\partial z} + f_z + \mu\,\nabla^2 u_z \quad (6)$$

Where u_r, u_θ, u_z are the velocities in the r, θ , z cylindrical coordinate directions, p is the pressure, f_r, f_θ are the body force components in the r, θ , z directions and the operators $\frac{D}{Dt}$ & ∇^2 are

$$\frac{D}{Dt} = \frac{\partial}{\partial t} + u_r\frac{\partial}{\partial r} + \frac{u_\theta}{r}\frac{\partial}{\partial \theta} + u_z\frac{\partial}{\partial z} \quad (7)$$

$$\nabla^2 = \frac{\partial^2}{\partial r^2} + \frac{1}{r}\frac{\partial}{\partial r} + \frac{1}{r^2}\frac{\partial^2}{\partial \theta^2} + \frac{\partial^2}{\partial z^2} \quad (8)$$

The following two equations determine the turbulent kinetic energy and specific dissipation rate of the conventional k-ω model respectively:

$$\frac{\partial}{\partial t}(\rho k) + \frac{\partial}{\partial x_i}(\rho k u_i) = \frac{\partial}{\partial x_j}\left(\Gamma_k \frac{\partial k}{\partial x_i}\right) + G_k - Y_k + S_k \quad (9)$$

$$\frac{\partial}{\partial t}(\rho \omega) + \frac{\partial}{\partial x_i}(\rho \omega u_i) = \frac{\partial}{\partial x_j}\left(\Gamma_\omega \frac{\partial \omega}{\partial x_j}\right) + G_\omega - Y_\omega + S_\omega \quad (10)$$

These equations, G_k illustrates how mean velocity gradients cause turbulence to produce kinetic energy. G_ω represents the generation of ω. Γ_k and represents the effective diffusivity of k and ω, respectively. Y_k and represent the dissipation of k and ω due to turbulence. S_k and are user-defined source terms. The impact on the overall structure of the flow field is controlled by a low Reynolds number correction factor, which is given as:

$$\alpha^* = \alpha^*_\infty \left(\frac{\alpha^*_0 + Re_t/R_k}{1 + Re_t/R_k}\right) \quad (11)$$

Where, $R_{et} = \frac{\rho k}{\mu \omega}$, R_k=6, $\alpha^*_0 = \frac{\beta_i}{3}$, $\beta_i = 0.072$, α^*_∞=1, Closure Coefficient for the Transitional k- ω Model are:- α^*_∞=1, α_∞=0.52, $\beta^*_\infty = 0.09, \beta_i = 0.072, R_k = 6$, and $R_\beta = 8$

The three main characteristics that describe blood flow via an artery are mass conservation, momentum conservation, and transfer of turbulence. The fluid (blood) is homogeneous, incompressible, and non-Newtonian. The mass density of blood is considered as 1060 Kgm^{-3}. The flow is considered as steady. The Standard k-ω model will be used for turbulence modeling.

- 2D
- Non-Newtonian, Incompressible & steady flow
- Rigid wall
- Reynolds number range 400 to 1500
- 35%, 50%, 75%, 86% & 95% stenosis region will be considered
-

3. Numerical Modelling

By designating the inlet flow as "velocity inlet" at the preset esteem and the output flow as "pressure outlet," boundary conditions are established. A healthy person has a systolic pressure of about 120 mmHg and a diastolic pressure of about 80 mmHg. As a result, 100 mmHg was chosen (about 13332 Pascal) as the static gauge pressure at the outlet by averaging the two phases' pressures.
The wall-designated boundary line was subjected to a stationary and no-slip condition **Fig.4** shows the boundary conditions.

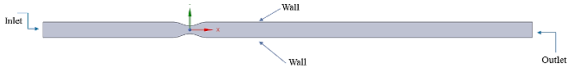

Fig.4 Boundary Condition of the geometry

The solution method for this simulation is that solving the equations coupled algorithm had been used as pressure velocity coupling. And for spatial discretization second order algorithm had been used for pressure, momentum, turbulence kinetic energy and specific dissipation rate. For the convergence of the simulations residuals absolute criteria had been taken as $1e^{-6}$.
Hemodynamic characteristics of the fluid must be set before the non-Newtonian Carreau model can be activated in ANSYS Fluent to create non-Newtonian fluid.

3.4 Model Validation

It was compared to the study of Ghalichi et al. (1998) [22] to validate the model. Wall shear stress as a function of Reynolds number at the stenotic neck Saad and Giddens (1983) [21] provided the original data for all the experimental measurements.

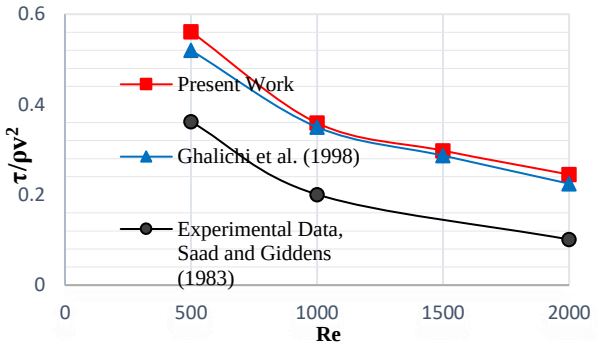

Fig.5 Model Validation

Fig.5 shows there is a deviation of present work from Ghalichi's work. For Re 500 the error is about 7.92%. For Re 1000 the error is about 2.67%, For Re 1500 the error is about 3.86% and for the Re 2000 the error is about 9.09%. There is a huge deviation with the experimental values of Saad and Giddens, but the trend of plot is identical.

4.0 Result and Discussion

Fig.6 shows that centerline static pressure distribution for various mesh sizes. The number of elements and nodes for various mesh sizes are given in **Table 3.**

Table 3 Number of elements and nodes for various Mesh

Mesh Name	Elements Number	Nodes Number
Mesh 0	27993	27060
Mesh 1	71500	72666
Mesh 2	94650	95988
Mesh 3	120700	122206
Mesh 4	149910	151584

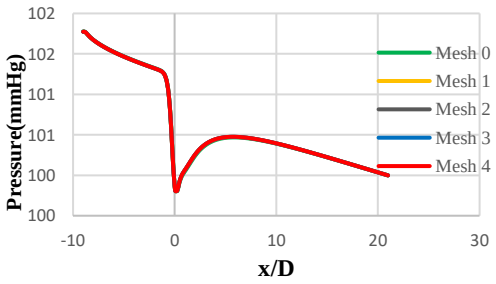

Fig.6 Centerline Pressure difference (number of elements)

The centerline static pressure distribution plot is deviated a bit for Mesh 0. But for the rest of the mesh sizes (Mesh 1-Mesh 4) the pressure distribution is identical. It suggests that the solution is grid-independent after Mesh 1 and onwards. And the simulation is carried out by setting the mesh elements 120700 and nodes 122206 which is Mesh 3 because of the smaller changes in Pressure values compared to Mesh 4(almost no change at all) than Mesh 2. The main aim being accurate results.

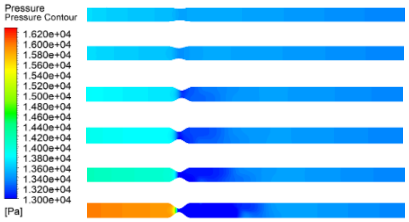

Fig.7 Static Pressure distribution contour for various stenosis (a) 35% (b) 50% (c) 75% (d) 80% (e) 86% and (f) 95%

Fig.7 demonstrates that the static pressure distribution is largest at the intake and least at the outflow. For the 95% stenosis, the pressure differential is extremely large (16000 Pa to 13000 Pa). Additionally, except for the area close to the stenosis, the fluctuation in pressure with respect to the length of the artery is linear. Pressure fluctuations near to the stenosis are deadly, given that the value of it is very high for 95% stenosis. In 35% stenosis a very little fluctuation of pressure is perceived in the artery, not fatal. In case of 50% the fluctuation increased but not that high. Fluctuation became much higher after 75% which is technically bad for health. After that at 86% and 95% the fluctuations became more than 1000 Pa worsening the condition.

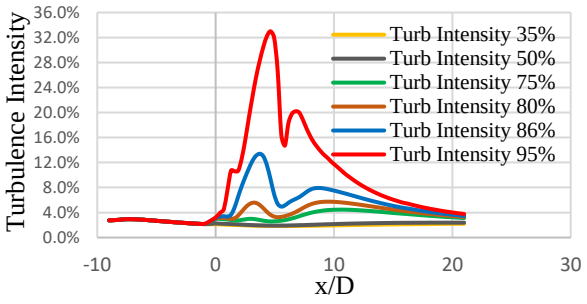

Fig.8 Turbulence Intensity for various stenosis (a) 35% (b) 50% (c) 75% (d) 80% (e) 86% and (f) 95%

Fig.8 shows that the turbulence intensity inside the artery for various blockage geometries. Since the ratio of the standard deviation of the fluctuating velocity to the mean velocity determines the severity of the turbulence. It evaluates how severe turbulence cases are. In 35% and 50% stenosed artery the turbulence is very less in the post stenotic region. As the stenosis increases the turbulence intensity in the post stenotic region is also increasing. It is also seen that the turbulence intensity occurs mostly where the streamline doesn't pass through (separation region). In higher stenosed blockage artery 75%, 80%, 86% and 95% the turbulence intensity is high (>5%) in the post stenotic region.

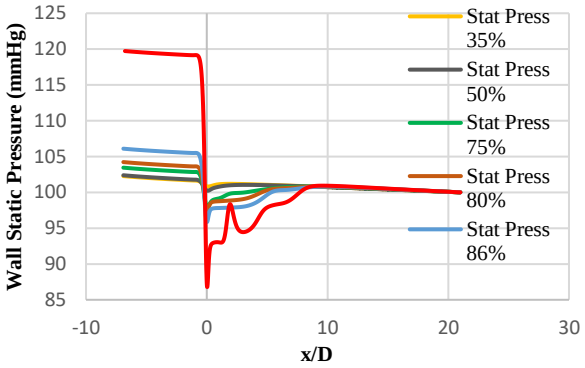

Fig.9 Wall static pressure for various stenosed percentages 35%, 50%, 75%, 80%, 86% and 95%

Fig.9 shows that wall static pressure at inlet is maximum and minimum at the outlet for all five geometries. Though the outlet pressure is same in all the models but there shows a significant change in inlet pressure. Higher the stenosed percentage the higher the inlet pressure is. The outlet pressure for all geometries is 100 mmHg which is average pressure of systole and diastole. But the inlet pressure of 95% stenosed artery is about 120 mmHg. So, there is a heavy fluctuation of pressure at the stenotic region which leads to fatal condition. In 35% and 50% the pressure fluctuation in stenotic region is mild. In the 85% stenosed artery this fluctuation isn't that much but still considerable. In 75% stenosed artery the fluctuation is 7 mmHg (1000 Pa). This is not so severe but growing from here can lead towards danger. In 95% artery some fluctuation is visible at post stenotic region. That's because of heavy turbulence and large vortex generation.

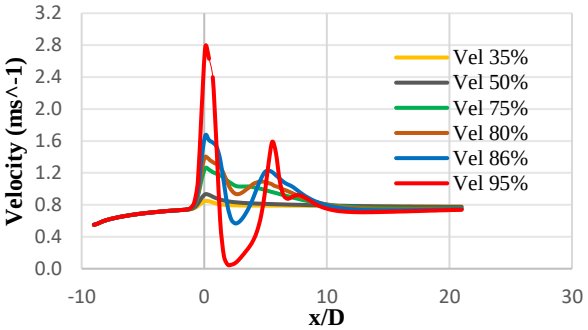

Fig.10 Velocity Profile for various stenosed percentages 35%, 50%, 75%, 80%, 86% and 95%

Fig. 10 shows that velocity fluctuation due to various obstruction geometries. The inlet velocity is same for all the models which is steady. The outlet velocity is almost same for all the models. There is a big increase in velocity in stenotic region for 95% stenosis. For 86% stenosis there is also a significant increase in velocity at stenosis. But for the other three models the velocity increase isn't that much significant. That's because of the pressure drop in the stenotic region. Cause pressure and velocity have proportional relation. The static pressure fluctuation is more at stenosed area. So, velocity also fluctuated reversely. The velocity fluctuation at post stenotic region

is seen for 95% and 86% stenosis as well. At post stenotic region for higher blockage geometries velocity trend moves erratically from centerline for a certain period.

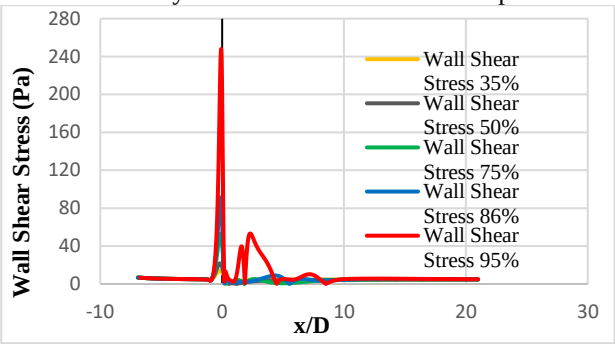

Fig.11 Wall Shear Stress for various stenosed percentages 35%, 50%, 75%, 80%, 86% and 95%

Fig.11 shows that variation of wall shear stress. Since the severity of stenosis increases, the WSS also increase, and the maximum variation is dominated by 95%. The pre stenotic region has a modest increase in shear stress while increasing dramatically in the proximal stenotic area. Whereas it reduces further in the distal stenotic and post stenotic region. This reduction in shear stress boosts the production of reactive oxygen species, which in turn boosts LDL oxidation in the intima. The result obtained from 35% and 50% stenosis agrees well with the clinical observation and the result for 75% isn't considered much severe but still injurious to health. The critical stenosis can be considered as 80% based on the above findings. Given that it is lethal for 80% of arteries, the pressure variation near to the stenosis is highly significant. as shown in **Fig.12** The fluctuation of pressure is about 14000 Pa to 13000 Pa. This high pressure in the pre stenosis region can very well damage the artery wall in pre stenosis area.

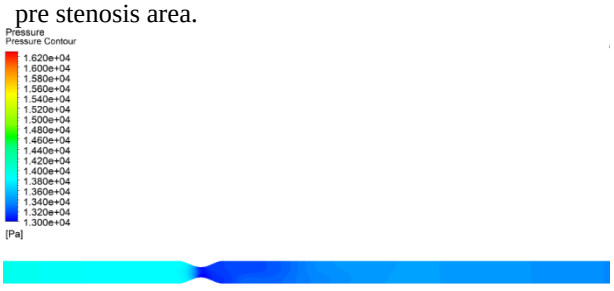

Fig.12 Static Pressure Distribution for 80% stenosed artery

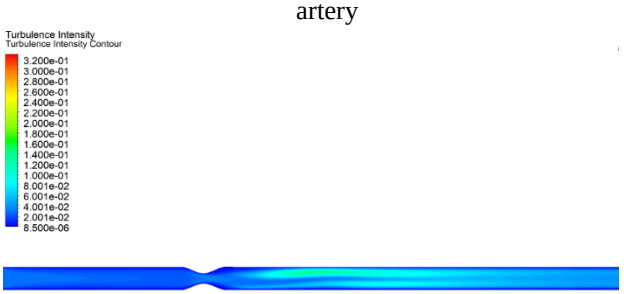

Fig.13 Turbulence Intensity Contour for 80% stenosis

In **Fig.13** shows that the turbulence intensity at the post stenotic region is high enough to cause trouble. For this turbulence vortex length is also increased which is abnormal for blood flow through an artery.

Fig.14 shows that the wall shear stresses the pre stenotic throat dramatically increased up to 50 Pa which can damage the artery wall and cause rapture in the pre stenotic region.

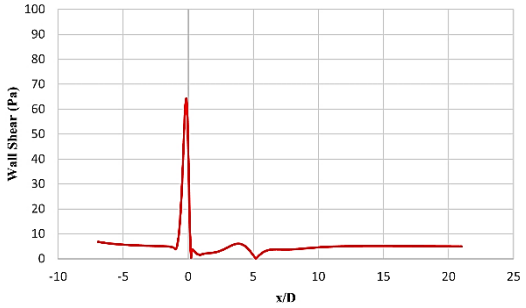

Fig.14 Wall Shear Stress for 80% stenosis artery

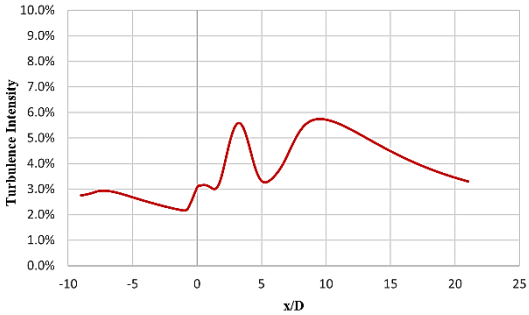

Fig.15 Turbulence Intensity for 80% stenosis artery

Fig.15 shows that the turbulence intensity at the post stenotic region rise above 5% which exceeds medium turbulence limit is very abnormal for blood flow through an artery. It can cause troubles to a human being.

5.Conclusion

In this work, a Carreau model of blood flow through a stenosed artery was validated (assuming fluid to be non-Newtonian) and simulated through varying blockages-35%, 50%, 75%, 80%, 86% and 95%.

i. It is seen that blood flow switches from laminar to turbulent at post stenotic region.

ii. The turbulence intensity increases with the stenosis percentage and as severity increases the velocity and shearing stress increase in the stenosed area. The most stress being imposed in the stenosed area.

iii. Turbulence intensity goes past medium turbulence limits for 80% stenosis and more than that. From velocity values 75 % blockage is inconvenient to health and 80% stenosis can be considered critical Anything higher would cause serious trouble decreasing blood supply (95% - fatal).

Thus, a closer inspection of the critical stenosis percentage shows how the various parameters indicate the change and measuring those can help predict the condition of cardiovascular systems. The investigation answers the main question of interest here that from above 75% condition warrants surgery and below might in some cases allow therapeutics only.

Some extensions to the work need to be considered for further analysis. The fluid-structure interactions (FSI)

could be applied to the model also blood velocity changes with time for different cardiac cycles can be considered for more accurate and realistic simulation of the stenosis can be considered while simplifying other parameters. Also, patient-specific medical imaging technique based real geometries of stenosis, extracted from patient MRI images could be used for more reliable patient health support in detecting the severity of condition.

6. References

[1] S. J. George and J. Johnson, "Atherosclerosis: molecular and cellular mechanisms," p. 398, 2010.

[2] V. Deplano, Y. Knapp, E. Bertrand, and E. Gaillard, "Flow behaviour in an asymmetric compliant experimental model for abdominal aortic aneurysm," *J Biomech*, vol. 40, no. 11, pp. 2406–2413, 2007, doi: 10.1016/J.JBIOMECH.2006.11.017.

[3] S. A. Berger and L. D. Jou, "Flows in Stenotic Vessels," *https://doi.org/10.1146/annurev.fluid.32.1.347*, vol. 32, pp. 347–382, Nov. 2003, doi: 10.1146/ANNUREV.FLUID.32.1.347.

[4] M. S. Moayeri and G. R. Zendehbudi, "Effects of elastic property of the wall on flow characteristics through arterial stenoses," *J Biomech*, vol. 36, no. 4, pp. 525–535, Apr. 2003, doi: 10.1016/S0021-9290(02)00421-9.

[5] M. A. Zulliger, P. Fridez, K. Hayashi, and N. Stergiopulos, "A strain energy function for arteries accounting for wall composition and structure," *Journal of Biomechanics*, vol. 37, no. 7, pp. 989–1000, Jul. 2004, doi: 10.1016/J.JBIOMECH.2003.11.026.

[6] T. Matsumoto, T. Goto, T. Furukawa, and M. Sato, "Residual stress and strain in the lamellar unit of the porcine aorta: Experiment and analysis," *Journal of Biomechanics*, vol. 37, no. 6, pp. 807–815, Jun. 2004, doi: 10.1016/J.JBIOMECH.2003.08.014.

[7] W. Shyy, M. Francois, H. S. Udaykumar, N. N'dri, and R. Tran-Son-Tay, "Moving boundaries in micro-scale biofluid dynamics,"*Applied Mechanics Reviews*, vol. 54, no. 5, pp. 405–452, Sep. 2001, doi: 10.1115/1.1403025.

[8] M. Bathe and R. D. Kamm, "A fluid-structure interaction finite element analysis of pulsatile blood flow through a compliant stenotic artery," *Journal of Biomechanical Engineering*, vol. 121, no. 4, pp. 361–369, 1999, doi: 10.1115/1.2798332.

[9] D. Tang, C. Yang, and D. N. Ku, "3-D thin-wall model with fluid-structure interactions for blood flow in carotid arteries with symmetric and asymmetric stenoses," *Computers and Structures*, vol. 72, no. 1, pp. 357–377, 1999, doi: 10.1016/S0045-7949(99)00019-X.

[10] C. Clark, "Turbulent velocity measurements in a model of aortic stenosis," *Journal of Biomechanics*, vol. 9, no. 11, pp. 677–687, 1976, doi: 10.1016/0021-9290(76)90169-X.

[11] M. D. Deshpande and D. P. Giddens, "Turbulence measurements in a constricted tube," *Journal of Fluid Mechanics*, vol. 97, no. 1, pp. 65–89, 1980, doi: 10.1017/S0022112080002431.

[12] S. A. Ahmed and D. P. Giddens, "Velocity measurements in steady flow through axisymmetric stenoses at moderate Reynolds numbers," *Journal of Biomechanics*, vol. 16, no. 7, 1983, doi: 10.1016/0021-9290(83)90065-9.

[13] S. A. Ahmed and D. P. Giddens, "Pulsatile poststenotic flow studies with laser Doppler anemometry," *Journal of Biomechanics*, vol. 17, no. 9, pp. 695–705, 1984, doi: 10.1016/0021-9290(84)90123-4.

[14] F. Ghalichi, X. Deng, A. de Champlain, Y. Douville, M. King, and R. Guidoin, "Low Reynolds number turbulence modeling of blood flow in arterial stenoses," *Biorheology*, vol. 35, no. 4–5, pp. 281–294, 1998, doi: 10.1016/S0006-355X(99)80011-0.

[15] "Effect of increased severity in patient specific stenosis of common carotid artery using CFD-a case study — Manipal Academy of Higher Education, Manipal,India."https://manipal.pure.elsevier.com/en/publications/effect-of-increased-severity-in-patient-specific-stenosis-of-comm (accessed Apr. 04, 2022).

[16] C. Tu and M. Deville, "Pulsatile flow of non-Newtonian fluids through arterial stenoses," *Journal of Biomechanics*, vol. 29, no. 7, pp. 899–908, Jul. 1996, doi: 10.1016/0021-9290(95)00151-4.

[17] A. Razavi, E. Shirani, and M. R. Sadeghi, "Numerical simulation of blood pulsatile flow in a stenosed carotid artery using different rheological models," *J Biomech*, vol. 44, no. 11, pp. 2021–2030, Jul. 2011, doi: 10.1016/J.JBIOMECH.2011.04.023.

[18] R. Ellahi, S. U. Rahman, M. Mudassar Gulzar, S. Nadeem, and K. Vafai, "A mathematical study of non-Newtonian micropolar fluid in arterial blood flow through composite stenosis," *Applied Mathematics and Information Sciences*, vol. 8, no. 4, pp. 1567–1573, Jul. 2014, doi: 10.12785/AMIS/080410.

[19] S. Karimi, M. Dadvar, M. Dabagh, P. Jalali, H. Modarress, and B. Dabir, "Simulation of Pulsatile Blood Flow through Stenotic Artery Considering Different Blood Rheologies: Comparison of 3D and 2D-Axisymmetric Models," vol.25, no.2, Apr.2013.http://dx.doi.org/10.4015/S1016237213500233,

[20] A. Harloff, T. Zech, F. Wegent, C. Strecker, C. Weiller, and M. Markl, "Comparison of blood flow velocity quantification by 4D flow MR imaging with ultrasound at the carotid bifurcation," *AJNR Am J Neuroradiol*, vol. 34, no. 7, pp. 1407–1413, Jul. 2013, doi: 10.3174/AJNR.A3419.

[21] N. Saleem, T. Hayat, and A. Alsaedi, "A Hydromagnetic Mathematical Model For Blood Flow Of Carreau Fluid," http://dx.doi.org/10.1142/S1793524514500107,vol. 7, no.1,Feb 2014,doi:10.1142/S17935245145001

[22] F. B. Tian, L. Zhu, P. W. Fok, and X. Y. Lu, "Simulation of a pulsatile non-Newtonian flow past a stenosed 2D artery with atherosclerosis," *Comput Biol Med*, vol. 43, no. 9, pp. 1098–1113, Sep.2013, doi: 10.1016/J.COMPBIOMED.2013.05.023.
[23] S. P. Shupti, M. M. Molla, and M. Mia, "Pulsatile Non-Newtonian Fluid Flows in a Model Aneurysm with Oscillating Wall," *Front Mech Eng*, vol. 3, Nov. 2017, doi: 10.3389/FMECH.2017.00012.
[24] G. Lorenzini and E. Casalena, "CFD analysis of pulsatile blood flow in an atherosclerotic human artery with eccentric plaques," *J Biomech*, vol. 41, no. 9, pp. 1862–1870, 2008, doi: 10.1016/J.JBIOMECH.2008.04.009.
[25] M. X. Li, J. J. Beech-Brandt, L. R. John, P. R. Hoskins, and W. J. Easson, "Numerical analysis of pulsatile blood flow and vessel wall mechanics in different degrees of stenoses," *J Biomech*, vol. 40, no. 16, pp. 3715–3724, 2007, doi: 10.1016/J.JBIOMECH.2007.06.023.
[26] F. Ghalichi, X. Deng, A. de Champlain, Y. Douville, M. King, and R. Guidoin, "Low Reynolds number turbulence modeling of blood flow in arterial stenoses," *Biorheology*, vol. 35, no. 4–5, pp. 281–294, 1998, doi: 10.1016/S0006-355X(99)80011-0.
[27] Ali Ostadfar, Biofluid Mechanics Principles and Applications, Academic Press (Elsevier),2016.

NOMENCLATURE

WSS	Wall Shear Stress
k	Turbulent Kinetic Energy
ω	Specific Dissipation Rate
D	Diameter of Artery
2D	Two Dimensional
Re	Reynolds Number
x	Axial location of the flow field
ρ	Density of Blood
τ	Shearing Stress
γ	Shear Rate
r	Stenosed Throat Radius